J. Biochem. **135**, 33–42 (2004)
DOI: 10.1093/jb/mvh004

Instability of the Apo Form of Aromatic L-Amino Acid Decarboxylase *In Vivo* and *In Vitro*: Implications for the Involvement of the Flexible Loop That Covers the Active Site

Nahoko Matsuda[1], Hideyuki Hayashi[2], Shinichi Miyatake[1], Toshihiko Kuroiwa[1] and Hiroyuki Kagamiyama[*,2]

[1]Department of Neurosurgery and [2]Department of Biochemistry, Osaka Medical College, 2-7 Daigakumachi, Takatsuki 569-8686

Received September 23, 2003; accepted October 29, 2003

Pyridoxine deficiency caused a decrease in the amount of aromatic L-amino acid decarboxylase (AADC) in PC12 cells to less than 5% of the control. The degree of the enzyme saturation with the coenzyme pyridoxal 5′-phosphate (PLP) was around 90% for both the control and the pyridoxine-deficient cells, contrary to earlier reports by others. Mathematical analysis of the result indicated that the AADC apoenzyme is degraded at least 20-fold faster than the holoenzyme in the cells. To determine the mechanism of the preferential degradation of the apoenzyme, *in vitro* model studies were carried out. AADC has a flexible loop that covers the active site. This loop was easily leaved by proteases at similar rates for both the holoenzyme and the apoenzyme. However, in the presence of the substrate analog, dopa methyl ester, the holoenzyme was not cleaved by proteases, while the apoenzyme was cleaved similarly. These results indicated that the ligand that forms a Schiff base (aldimine) with PLP is fixed to the active site and stabilizes the flexible loop. The structure of the rat AADC–dopa complex modeled on the crystal structure of pig AADC showed that the flexible loop can fit in the concave surface at the entrance of the active site, its aliphatic and aromatic residues forming hydrophobic interactions with the substrate catechol ring. It was postulated that the flexible loop of the holoenzyme is stabilized *in vivo* by taking a closed structure that holds the PLP–substrate aldimine, while the apoenzyme cannot bind the substrate and its flexible loop is easily cleaved, leading to the preferential degradation of the apoenzyme.

Key words: apoenzyme, aromatic-l-amino-acid-decarboxylase, decarboxylation, proteolysis, pyridoxal-phosphate, transamination.

Abbreviations: AADC, aromatic L-amino acid decarboxylase [EC 4.1.1.28]; CD, circular dichroism; K–P_i, potassium phosphate buffer; PIPES, piperazine-1,4-bis(2-ethanesulfonic acid); PLP, pyridoxal 5′-phosphate; PMP, pyridoxamine 5′-phosphate.

Pyridoxal 5′-phosphate (PLP) enzymes are a group of enzymes that catalyzes various reactions of amino acids (*1*). The activities of the enzymes are strictly dependent on the coenzyme PLP, which forms the catalytic center of PLP enzymes. Thus, the apo form of a PLP enzyme is totally inactive. It has been reported that the deficiency of pyridoxine (vitamin B_6), the precursor form of PLP, leads to decrease in the holo form of the enzyme and the product of the enzymatic reaction (*2*).

In addition to its importance in catalysis, PLP may be involved in maintaining the integrity of PLP enzymes. The pyridoxine-deficiency studies also showed that the content of not only the holoenzyme but also the total enzyme (holoenzyme plus apoenzyme) is decreased in some PLP enzymes (*3*, *4*), indicating the role of PLP in the *in vivo* stabilization of PLP enzymes. The precise mechanism of this effect of PLP is yet to be clarified. One hypothesis assumes the presence of a protease that specifically recognizes the apo form of the enzymes (*5*). However, PLP is usually buried in the interior of the enzyme protein, and it is hard to explain how the presence or absence of PLP at the active site can be recognized by other proteins.

AADC is a PLP enzyme that catalyzes the irreversible decarboxylation of several aromatic L-amino acids, including dopa (3,4-dihydroxyphenylalanine), *m*-tyrosine, *p*-tyrosine, phenylalanine, 5-hydroxytryptophan, and tryptophan (*6*). Among them, the decarboxylation products of dopa and 5-hydroxytryptophan, dopamine and serotonin, respectively, are known as important neurotransmitters. The activity of AADC, therefore, has important meanings in discussing the physiology and pathophysiology of neurotransmission, including Parkinson's disease. Although systemic pyridoxine deficiency is a rare disease, local deficiency of pyridoxine in the central nervous system is not uncommon. For example, treatment with drugs containing hydrazino groups, such as the antimicrobial agent isoniazid (isonicotinic acid hydrazide), is known to cause convulsion by decreasing

*To whom correspondence should be addressed. Tel: +81-72-683-1221 Ext. 2645, Fax: +81-72-684-6516, E-mail: med001@art.osaka-med.ac.jp

the γ-aminobutyrate content (*7*). Thus, the activity of AADC should also be understood with reference to PLP.

As a first step to study this point, we examined the stability of aromatic L-amino acid decarboxylase (AADC) both *in vivo* and *in vitro*. The results showed that, contrary to the earlier observations by others, the apoenzyme occupies only a small part of the AADC protein even in the pyridoxine-depleted condition, suggesting that the apoenzyme is degraded faster than the holoenzyme *in vivo*. The *in vitro* model study suggested the involvement of the flexible loop that covers the active site of AADC in the degradation of the enzyme inside the cell. The physiological significance of the AADC degradation in the cells is also discussed in the light of the recent finding of the role of catechol compounds in the pathogenesis of Parkinson's disease.

MATERIALS AND METHODS

Materials—PC12 cells were purchased from Dainippon Pharmaceutical (Osaka). Gibco™ DMEM (11965) without pyridoxine hydrochloride was from Invitrogen (Carlsbad, CA).

Purification of AADC and Preparation of the Apoenzyme—AADC was purified as described previously (*6*, *8*). The coenzyme PLP was removed from AADC as a phenylhydrazone according to the method described in ref. 6 with modifications. To the holoenzyme in 0.9 ml of 50 mM PIPES, pH 7.0, was added 0.1 ml of 50 mM phenylhydrazine hydrochloride (pH adjusted to 7.0 with NaOH). The solution was kept at 37°C for 30 min, then passed through Sephadex G-25 (15 mm × 52 mm) equilibrated with 0.5 M potassium phosphate buffer (K–P_i), pH.8.0. The gel filtration process was repeated twice to obtain the apo form of AADC. This procedure removed more than 95% of PLP from AADC (determined spectroscopically) without significant denaturation of the enzyme.

Spectroscopic Measurements—Absorption spectra were taken in a Hitachi U-3300 spectrophotometer at 25°C. Circular dichroism (CD) spectra were taken in a JASCO J-720WI spectropolarimeter at 25°C, using a 1 mm pathlength cell. Scan parameters were: band width, 1 nm; step resolution, 0.2 nm; response, 2 s; speed, 20 nm·min^{-1}; accumulation, 3. The spectrum of the buffer solution with or without the ligand dopa methyl ester was subtracted.

Determination of the Protein Concentration—The concentration of AADC in solution was determined spectrophotometrically. The apparent molar extinction coefficients used were 7.75×10^4 M^{-1}·cm^{-1} for the apoenzyme and 7.90×10^4 M^{-1}·cm^{-1} for the holoenzyme at 280 nm (*6*). Protein concentrations of the cell extracts were determined by the Bradford method (*9*).

Limited Proteolysis with Trypsin—AADC was incubated with 1/1000 (w/w) amount of L-1-chloro-3-(4-tosylamido)-4-phenyl-2-butanone-treated trypsin in 50 mM PIPES–NaOH, pH 7.0, at 25°C and the digestion was stopped by the addition of a twofold weight (relative to trypsyn) of soybean trypsin inhibitor.

Electrophoresis—Dodecyl sodium sulfate (SDS) electrophoresis was performed on 12.5% polyacrylamide slab gels according to the method of Laemmli (*11*). Gels were stained with Coomassie Brilliant Blue R-250.

Cell Culture—PC12 cells were grown in DMEM high glucose (Gibco) supplemented with 5% fetal bovine serum (Sigma-Aldrich, St. Louis, MO) and 10% horse serum (Gibco) in 75-mm collagen-coated flasks at 37°C in an atmosphere of 5% CO_2 and 100% humidity. After replating onto 15-mm collagen-coated flasks, cells were cultured for 3 days and 6 days. Control cells were cultured in DMEM high glucose supplemented with 5% fetal bovine serum. Pyridoxine-depleted cells were grown in DMEM high glucose without pyridoxine with 5% fetal bovine serum and 20 mM 4-deoxypyridoxine. The medium was replaced 3 times a week. For the AADC activity measurements, cells were harvested at 0, 3, and 6 days.

AADC Activity—AADC activity was measured as described previously (*6*, *10*). The reaction mixture (1 ml) contained 0.1 M K–P_i, pH 7.0, 0.1 mM dithiothreitol, 5 μM PLP, and the enzyme. The reaction was started by adding dopa (final 0.5 mM). After incubation at 37°C, the reaction was stopped by the addition of 10 μl of 5 mM benzyloxyamine (*12*). The amount of dopamine formed was determined by use of an HPLC system LC-6A (Shimadzu, Kyoto) equipped with an electrochemical detector model ECD-300 (Eicom, Kyoto). The reaction mixture (usually 50 μl) was injected onto an Econopack C18 reversed phase column (4.5 mm × 150 mm), the temperature of which was maintained at 30°C with a waterbath. The mobile phase was 0.1 M K–P_i, pH 3.45, containing 5 mM octyl sodium sulfate, 48 μM EDTA, and 12.5% methanol (v/v). The flow rate was 1 ml·min^{-1}. Dopamine elution was monitored by the electrochemical detector, the potential being set to 450 mV relative to the Ag/AgCl reference electrode (*13*). The peak area was measured using System Gold (Beckman Coulter, Fullerton, CA) and the amount of dopamine was calculated by comparing it with the peak area of the standard compound.

For determination of AADC activity in PC12 Cells, the harvested cells from 10 ml of culture were suspended in 50 μl of 1 mM K–P_i, pH 7.0, containing 0.2% (w/w) polyoxyethylene octyl phenyl ether (Triton X-100), 25-times diluted protease inhibitor cocktail (Sigma-Aldrich) and 0.1% (v/w) soybean trypsin inhibitor, and sonicated for 2 min at a power level of 50 in a Branson Ultrasonic (Danbury, CT) Sonifier Cup Horn. An aliquot of 20 μl of supernatant was used for measuring activity as described above.

Immunoblotting—PC12 cell extracts were analyzed by immunoblotting using a polyclonal antibody against AADC. The samples (10 μl of the supernatant described above) were separated by SDS-PAGE (12.5% polyacrylaminde), transferred to a nitrocellulose membrane, and sequentially incubated with the polyclonal rabbit anti-AADC IgG antibody and goat anti-rabbit IgG antibody conjugated with alkaline phosphatase. This analysis was carried out using an Immunoblot Kit GAR-AP (Bio-Rad, Hercules, CA).

Degree of AADC Saturation with PLP in the PC12 Cells—PC12 cells were disrupted as above. The cell extract (50 μl) was diluted to 0.4 ml with 1 mM K–P_i and divided into two equal volumes (extract I and II). To extract II was added 1 μl of 1 mM PLP (final 5 μM), and the two extract solutions were incubated for 30 min at room temperature, then applied to PD-10 columns equilibrated with 50 mM PIPES, pH 7.0. The fraction eluted at

2.75–4.25 ml containing AADC was collected and 100 μl of 0.1 mM dithiothreitol was added. An aliquot of 950 μl was transferred to another test tube, and 50 μl of 10 mM dopa was added. After 30 min of incubation at 37°C, 10 μl of 5 mM benzyloxyamine was added. The amounts of dopamine formed in the solutions were measured as described above. The holoenzyme ratio was calculated as (the amount of dopamine formed from extract I)/(the amount of dopamine formed from extract II).

Determination of the Cytosolic PLP Concentration—The intracellular PLP content was determined as described by Tsuge (*14*). PC12 cell extracts were deproteinized with 1 M perchloric acid and adjusted to pH 7.5 with KOH. Then 20 μl of 0.5 M KCN was added, and the solution was agitated at 50°C for 3 h. The resulting solution was adjusted to pH 3.5 with HCl and injected onto an Econopack C18 reversed phase column. The mobile phase was 0.1 M perchloric acid and 0.1 M sodium phosphate, pH 3.5, with a flow rate of 0.5 ml·min^{-1}. Fluorescence at 420 nm with excitation at 320 nm was monitored.

Structural Modeling—Modeling of rat AADC on the crystal structure of pig AADC (*15*) was carried out on MOE (Version 2003.02, Chemical Computing Group, Montreal, Canada) according to the manufacturer's instructions. Rat AADC has 85% amino acid identity with pig AADC and lacks the C-terminal 6 residues of pig AADC. After the sequences had been aligned, the residues of rat AADC were fitted to the coordinate data of pig AADC (1JS6). The coordinate data is missing residues 328–339 and the C-terminal 10 residues. Therefore, residues 328–339 and the C-terminal 4 residues of rat AADC were modeled without the coordinate data. MM energy minimization was done using Engh–Huber parameters. The PLP–dopa aldimine structure was built on 3-{[(3-hydroxy-2-methyl-5-phosphonooxymethyl-pyridin-4-ylmethyl)-amino]-2-methyl-propyl}-phosphonic acid (product aldimine) of the crystal structure of the *Salmonella* phosphothreonine decarboxylase (1LC8), which was superimposed on the structure of rat AADC obtained as above. The aldimine structure was energy-minimized using MMFF94s with all the residues of rat AADC being fixed except for His192 and Lys303 that directly interact with the PLP–dopa aldimine. The flexible loop (residues 328–345) was manually moved to fit in the concave surface at the entrance of the active site and subjected to energy-minimization using AMBER94. The *cis* bonds in the resulting structure were changed to *trans* bonds, and the entire structure was energy-minimized to obtain the final structure.

RESULTS AND DISCUSSION

Pyridoxine Depletion Decreases the Content of AADC in PC 12 Cells—PC12 cells were cultured either in the presence or absence of pyridoxine. At days 3 and 6 of cell culture, the intracellular pyridoxal 5′-phosphate (PLP) content of the pyridoxine-depleted cells decreased to 40% of the values of pyridoxine-supplemented cells (Fig. 1A). This reduction in the PLP content is similar to that reported by others (*16*). Concomitant with the decrease in the PLP content, the AADC activity markedly decreased

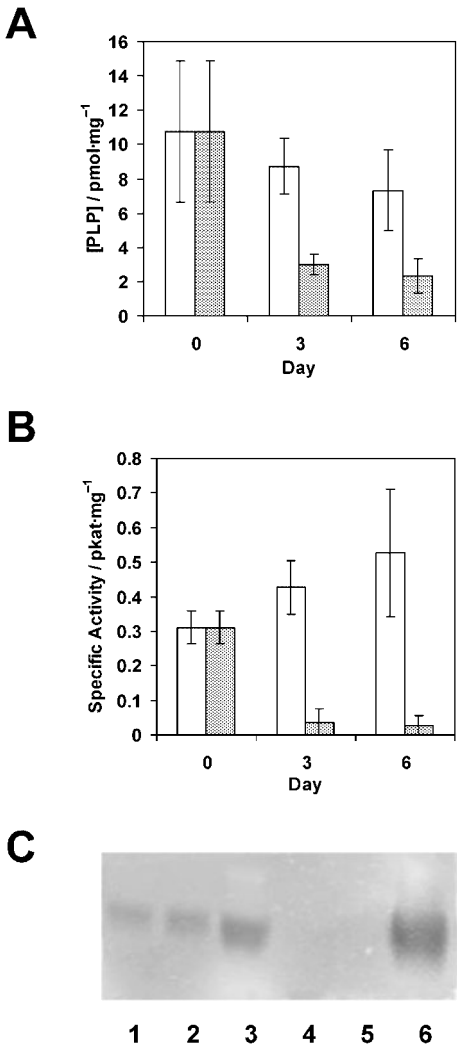

Fig. 1. **Changes in the PLP and AADC contents of PC12 cells on pyridoxine depletion.** (A) Intracellular PLP concentration of the pyridoxine-supplemented and -depleted cells, expressed in pmol per mg wet weight of the cells. Open, pyridoxine-supplemented cells; hatched, pyridoxine-depleted cells. Bars represent S.D. (B) AADC activity of the pyridoxine-supplemented and -depleted cells, expressed in pkat per mg wet weight of the cells. Open, pyridoxine-supplemented cells; hatched, pyridoxine-depleted cells. Bars represent S.D. (C) Immunoblotting of AADC in the pyridoxine-supplemented and -depleted cells. Lanes 1–3, control cells at 0, 3, and 6 days. Lanes 4–5, pyridoxine-depleted cells at 3 and 6 days. Lane 6, AADC (1 μg).

to 9% (day 3) and 5% (day 6) of the corresponding values of the pyridoxine-supplemented cells (Fig. 1B). The activities were measured in the presence of a saturating concentration of PLP (5 μM). Therefore, the values represent the amount of the intact (active) species of AADC. To determine whether an inactive form of AADC is present, the cell lysates were analyzed by immunoblotting. The amount of the immunologically detected AADC protein in the pyridoxine-supplemented cells increased with time (Fig. 1C), corresponding to the gradual increase in the AADC activity (Fig. 1B). On the other hand, the amount of AADC protein was below the detection limit in the pyridoxine-depleted cells at days 3 and 6. These results

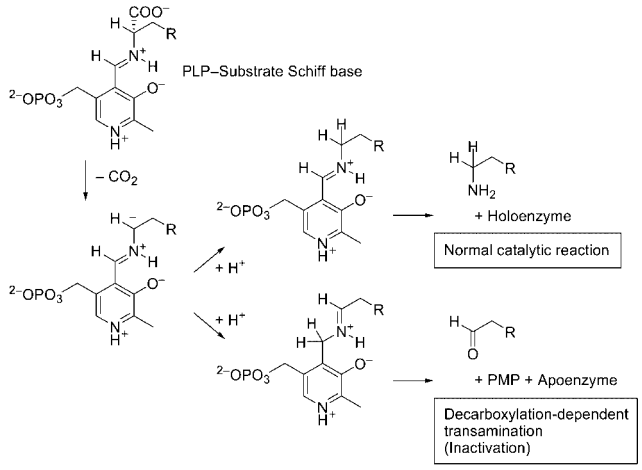

Scheme 1.

indicate that the AADC activities shown in Fig. 1B represent the amount of the AADC protein, and that AADC present in the PC12 cells is apparently in the intact, active form. Thus, pyridoxine deficiency decreases the amount of the AADC protein without accumulation of the inactive form of the enzyme.

Evaluation of the Degree of the Enzyme Saturation with PLP—The AADC activities shown in Fig. 1B represent the sum of the holoenzyme and the apoenzyme that can be converted to the holoenzyme. Therefore, it is important to measure separately the contents of the holoenzyme and the apoenzyme, *i.e.*, the degree of saturation of the enzyme with PLP.

Traditionally, the degree of the enzyme saturation with PLP has been assessed by comparing the activity of the enzyme in the absence of PLP with that in the presence of PLP. This method is based on the assumption that the former represents the holoenzyme and the latter the total enzyme (apoenzyme plus holoenzyme) present in the sample, because the apoenzyme is totally inactive. However, this method can only be applied to enzymes that bind PLP firmly and do not undergo side reactions. Decarboxylases are known to be prone to decarboxylation-dependent transamination, forming pyridoxamine 5′-phosphate (PMP), apoenzyme, and an aldehyde derived from the substrate (*17*; Scheme 1).

In the case of rat AADC, the ratio of the normal catalytic reaction to the decarboxylation-dependent transamination (partition ratio; R) is 1000 (*18*). The amount of holoenzyme decreases exponentially according to the equation $\exp(-(k_{cat}/R)t)$. As $k_{cat} = 5\ s^{-1}$ (*6*), the half life of the amount of holoenzyme is 2.3 min, much smaller than the incubation period generally used to measure the decarboxylase activity. Therefore, decarboxylases rapidly lose their activity in the absence of PLP. PMP is easily dissociated from decarboxylases to form the apoenzyme. In the presence of added PLP, the apoenzyme is rapidly converted to the holoenzyme, and by repeating the turnover, the enzyme retains full catalytic ability. Thus, the product formation increases linearly in the presence of PLP, but reaches saturation in the absence of PLP. Accordingly, the conventional method underestimates the extent of the enzyme saturation with PLP, and the deviation becomes more prominent as the incubation period for measuring the enzyme activity increases.

Table 1. **The Extent of Saturation of AADC with PLP in Pyridoxine (+) and Pyridoxine (–) PC12 Cells.**[a]

Extract from	Treatment	Dopamine formed (pmol)	Saturation with PLP
Pyridoxine (+) PC12	+PLP	31.8	91%
	–PLP	29.0	
Pyridoxine (–) PC12	+PLP	1.76	90%
	–PLP	1.58	

[a]Cells were harvested at day 6. Cell extracts were divided into two equal volumes, of which one was treated with PLP and the other was untreated, then both were gel-filtered. The total dopamine formed in 950 μl of the filtered extract solution was measured. Extracts from the cells in other cultivation media showed similar values, (90 ± 3)% for both pyridoxine (+) and pyridoxine (–) cells.

To overcome this problem, we have developed a method which is based on the fact that the content of the holoenzyme is proportional to the total amount of dopamine formed in the complete absence of PLP (*18*). Thus, the cell extract is divided into two portions of equal volume; to one of which is added excess PLP, thereby converting the apoenzyme to the holoenzyme. Then the two solutions are subjected to gel filtration to remove free PLP. Dopa is added to the solutions, and the reactions are allowed to proceed. The holoenzyme in each solution catalyzes the decarboxylation of dopa to form dopamine, but due to the decarboxylation-dependent transamination, essentially all the holoenzyme is converted to the apoenzyme within 30 min and no further formation of dopamine is observed (*18*). The maximum amount of dopamine, however, is proportional to the amount of the holoenzyme. Therefore, by comparing the maximum dopamine content in the two solutions, the enzyme saturation with PLP is determined. Using this method, saturation of AADC with PLP in rat liver has been determined to be around 90% (*18*), much higher than the previously obtained values (20–30%) by the conventional method (*2*, *19*, *20*). Nevertheless, the conventional method has still been used for discussing the apoenzyme/holoenzyme content of decarboxylases. For example, Kash *et al.* claimed that a large portion of the 65 k isoform of glutamate decarboxylase in mouse brain exists as the apoenzyme and that its activity is regulated by the intracellular PLP concentration, and from this study they proposed the concept of an "apoenzyme reservoir" (*21*). However, the low saturation with PLP appears to be an underestimation, and their results should be reinvestigated. We have applied this new, reliable method to estimate the saturation of AADC with PLP in both the pyridoxine-supplemented and -depleted PC12 cells as follows.

AADC Exists Predominantly as the Holoenzyme under Both the Pyridoxine-Supplemented and Depleted Conditions—The PC12 cell extract was either treated or not treated with PLP, passed through a PD-10 column to remove unbound PLP, and incubated with dopa. In the case of the pyridoxine-supplemented PC12 cells, the maximum amount of dopamine formed by the cell extract not pretreated with PLP was (90 ± 3)% of that of the cell extract pretreated with PLP (Table 1). That is, AADC is (90 ± 3)% saturated with PLP in the pyridoxine-supple-

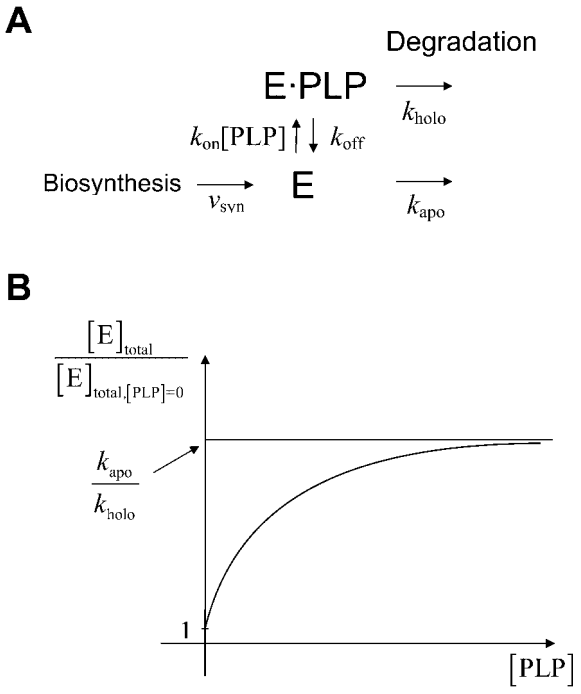

Fig. 2. **(A) Model of the degradation of AADC in the cell.** See text for details. **(B) Dependency of the total concentration of AADC on the concentration of PLP.** Drawn according to Eq. 4.

mented PC12 cells. The corresponding value in the case of the pyridoxine-depleted PC12 cells was again (90 ± 3)%, which is essentially identical to that of the pyridoxine-supplemented cells (Table 1). These results show that, AADC exists predominantly as the holoenzyme, irrespective of whether the PC12 cell is in the pyridoxine-supplemented or -depleted condition. This is in clear contrast with the report based on the conventional method that AADC in rat striatum is only 5–10% saturated with PLP under pyridoxine-restricted condition (*20*).

Degradation of the Apo Form of AADC Is Faster than the Holo Form—The findings that the apoenzyme accounts for only a small part of AADC in the pyridoxine-depleted condition and that the total amount of AADC is decreased by pyridoxine depletion suggest that the apoenzyme is degraded faster than the holoenzyme. To test this hypothesis, a mathematical analysis of the above results was carried out using the model shown in Fig. 2A. AADC is synthesized as the apo form at a rate of v_{syn}. The holo and the apo forms are degraded at different rates (k_{holo} and k_{apo}, respectively). At steady state, where the rate of formation is equal to the rate of breakdown, we can obtain the following equations:

$$k_{on}[PLP][E] = (k_{holo} + k_{off})[E{\cdot}PLP] \quad (1)$$

$$k_{off}[E{\cdot}PLP] + v_{syn} = (k_{on}[PLP] + k_{apo})[E] \quad (2)$$

where k_{on} and k_{off} are the association and dissociation rate constants for the PLP binding to the apoenzyme. Using Eqs. 1 and 2, the total concentration of the enzyme ($[E]_{total}$) is expressed as:

$$[E]_{total} = [E] + [E{\cdot}PLP] = \frac{k_{on}[PLP] + k_{off} + k_{holo}}{k_{holo} \cdot k_{on}[PLP] + (k_{off} + k_{holo})k_{apo}} v_{syn} \quad (3)$$

The ratio of $[E]_{total}$ at a concentration of PLP to $[E]_{total}$ in the absence of PLP ($[E]_{total,[PLP]=0}$) is:

$$\frac{[E]_{total}}{[E]_{total,[PLP]=0}} = \frac{k_{on}[PLP] + k_{off} + k_{holo}}{\frac{k_{holo}}{k_{apo}} k_{on}[PLP] + k_{off} + k_{holo}} \quad (4)$$

which is schematically shown in Fig. 2B. The ratio reaches a value of k_{apo}/k_{holo} with increasing [PLP]. This indicates that the content of the enzyme can vary less than (k_{apo}/k_{holo})-fold. Therefore, in order to explain the observation that $[E]_{total}$ decreases to 5% by pyridoxine depletion (Fig. 1B), the value of k_{apo}/k_{holo} must be larger than 20. Thus, the degradation of the apoenzyme is more than 20 times faster than that of the holoenzyme.

Structural Difference between the Apoenzyme and the Holoenzyme—The above results clearly show that the apoenzyme is preferentially degraded in PC12 cells. Therefore, the cells should have a mechanism that dis-

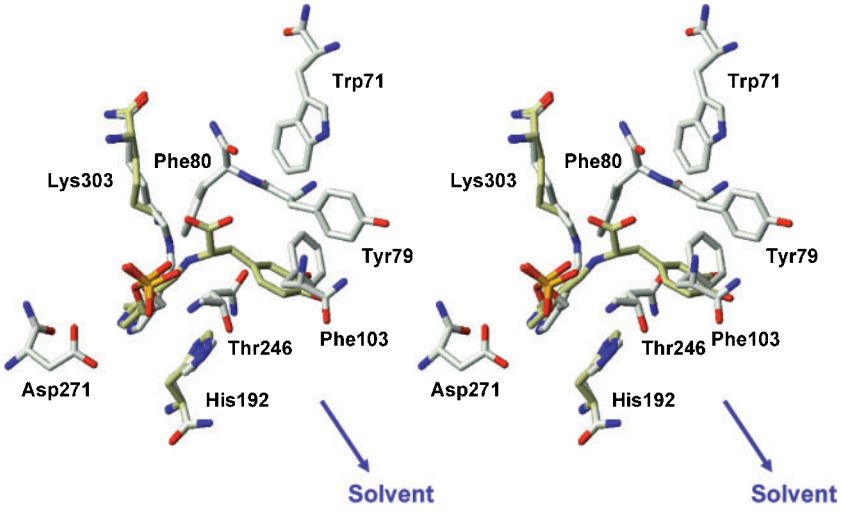

Fig. 3. **Structure of the proposed active site of rat AADC, prepared by homology modeling on the crystal structure of pig AADC (*15*).** The model of the PLP–dopa aldimine complex is superimposed (shown in khaki).

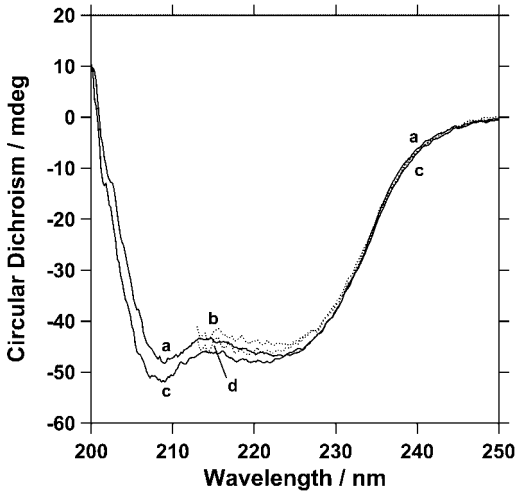

Fig. 4. **Circular dichroism spectra of 6.75 μM AADC in 50 mM K–P_i, pH 7.0.** a, holoenzyme; b, holoenzyme plus 1 mM DopaOMe; c, apoenzyme; d, apoenzyme plus 1 mM DopaOMe. Lines b and d are shown in dots. Spectra of b and d below 213 nm could not be obtained due to strong absorption of DopaOMe in this region. Therefore, the CD values at 222 nm, representing the helix content, were used in the discussion (see text).

criminates the apoenzyme from the holoenzyme. The CD spectra of the backbone region of the apoenzyme (Fig. 4, line c) is similar to that of the holoenzyme (Fig. 4, line a), indicating that there is no global conformational change between the apoenzyme and the holoenzyme. Rat AADC has 85% amino acid sequence identity with pig AADC. This enabled us to construct a model structure of rat AADC by homology modeling on the crystal structure of pig AADC (*15*). The active site is enlarged and is shown in Fig. 3. Apparently, PLP is buried in the interior of the protein; the solvent side of PLP is occupied by residues His192, Thr246, and Phe103. Therefore, it is an intriguing problem how the cellular protein degrading system can recognize the presence or absence of PLP at the active site. To explore the differential behavior of the apoenzyme and the holoenzyme toward proteases, a model study using limited trypsin digestion of AADC was carried out.

The Holoenzyme and the Apoenzyme Are Cleaved by Proteases but the Holoenzyme Is Protected in the Presence of a Substrate Analogue—Limited trypsin digestion was performed in the absence or presence of the substrate analogue dopa methyl ester (DopaOMe), which forms an external aldimine with PLP of AADC (*6*). DopaOMe was used instead of the substrate dopa because dopa is gradually decarboxylated to dopamine, which binds to AADC much less tightly than dopa (*22*), during the incubation period, which may make the interpretation of the results difficult. At steady state of the AADC-catalyzed decarboxylation of dopa, the external aldimine is the accumulating species (*8*). Therefore, the AADC–DopaOMe complex is considered to be a good model for the AADC–dopa complex. The presence of DopaOMe does not essentially affect the global conformation of the holoenzyme nor that of the apoenzyme, as judged from the CD value at 222 nm (Fig. 4). The holoenzyme and the apoenzyme were incubated with 1/1,000 (w/w) trypsin at 25°C in the presence

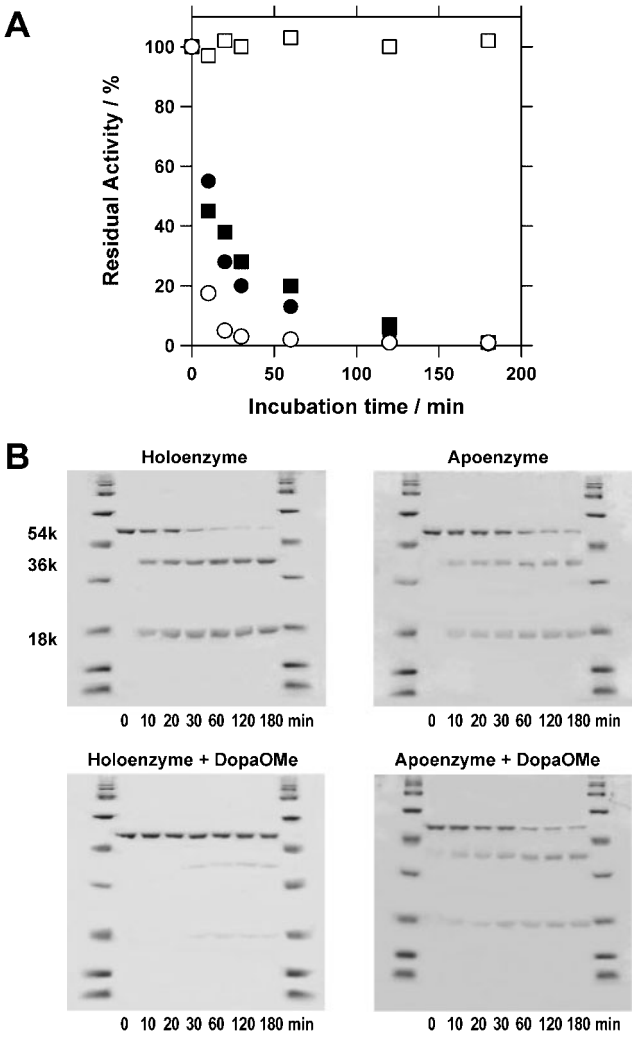

Fig. 5. **Time courses of the limited proteolysis of holo and apo AADC.** (A) AADC residual activity was measured at 0, 10, 20, 30, 60, 120, and 180 min. open circles, Holo AADC; open squares, Holo AADC in the presence of DopaOMe; solid circles, Apo AADC; solid squares, Apo AADC in the presence of DopaOMe. (B) SDS-PAGE analysis of the digested materials in A. Incubation times are indicated at the bottom. Molecular weight marker proteins at both ends are: myosin (rabbit muscle, 200 k), β-galactosidase (*E. coli*, 116 k), albumin (bovine serum, 66.2 k), ovalbumin (chicken egg white, 45.0k), carbonic anhydrase (bovine erythrocyte, 29.0 k), trypsin inhibitor (soybean, 20.1 k), lysozyme (chicken egg white, 14.4 k), and aprotinin (bovine lung, 6.50 k).

or absence of DopaOMe, and aliquots were taken at 0, 10, 20, 30, 60, 120 and 180 min and analyzed for AADC activity (Fig. 5A) and the covalent structure (SDS-PAGE analysis; Fig. 5B). Both the holo and the apo forms of AADC were inactivated rapidly; the residual activity reached almost zero after 30 min (Fig. 5A). In parallel with the inactivation, the 54 k subunit of AADC was cleaved to 36 k and 18 k polypeptides (Fig. 5B). The rate of inactivation and cleavage of the apoenzyme was slightly slower than that of the holoenzyme. In the presence of DopaOMe, however, the apoenzyme was similarly inactivated and cleaved, but the holoenzyme was stable even after 180 min, exhibiting a striking difference from the other three combinations (Fig. 5, A and B).

AADC is known to have a flexible loop that is easily attacked by proteases (*23*, *24*). In the X-ray crystallography of pig kidney AADC, residues Met328–Asp339 corresponding to the loop are invisible (*15*). Trypsin causes limited proteolysis of AADC at the peptide bond after Lys334 (pig AADC; *23*) and after Arg334 (rat AADC; *24*). This loop is also cleaved by chymotrypsin after Leu333 (*24*). These observations indicate that the loop containing Met328–Asp339 has high mobility and can be easily attacked by proteases to produce the 36 k and 18 k polypeptides. Analysis of the 18 k polypeptide of the cleaved apoenzyme (Fig. 5B) by automated Edman degradation showed that the cleavage site of the apoenzyme is the same as that of the holoenzyme. Similar results were obtained for chymotrypsin, which cleaves the bond at Leu333–Arg334 (data not shown). Thus, the flexible loop of the apoenzyme is easily cleaved by proteases in either the absence or presence of the ligand DopaOMe, but that of the holoenzyme is protected from proteases in the presence of DopaOMe, while it is similarly cleaved in the absence of the ligand.

Proposed Interaction between the Ligand and the Flexible Loop—DopaOMe forms an external aldimine with PLP of AADC (*6*). Therefore, it is expected that the apoenzyme cannot bind DopaOMe tightly, because the apoenzyme has no groups that could form covalent bonds with the amino group of the ligand. Accordingly, the above results of the limited tryptic digestion can be explained by assuming that the flexible loop interacts with DopaOMe and undergoes a large conformational change to form a rigid structure that is resistant to proteolysis.

The only known structure of a liganded AADC is that of the complex with carbidopa (*15*). However, carbidopa has an α-hydrazino group, whereas DopaOMe and dopa have an α-amino group. As the hydrazino group has one more N atom than the amino group, the PLP–carbidopa complex is expected to adopt a significantly different conformation from that of the PLP–dopa or PLP–DopaOMe complex. In fact, the side chain of carbidopa points toward the interior of the protein, in the opposite direction to the side chain of the ligands observed for other decarboxylases belonging to the same subfamily as AADC (*25*, *26*). Therefore, we constructed the model of the dopa-liganded structure shown in Fig. 3 based on the crystal structure of phosphothreonine decarboxylase complexed with its product aminopropanol phosphate (*26*), in which the side chain phosphoryl group of the product is pointed toward the *re* face (opposite to the former PLP-binding lysine residue, Lys303). Dopa fitted excellently to the structure of AADC, and the catechol ring is surrounded by aromatic residues Phe103, Tyr79, Trp71 and Phe80 (Fig. 3, khaki). These residues are considered to accept the side chain of dopa by hydrophobic interaction. However, a part of the catechol ring is exposed to the solvent in this modeled structure. This is expected from the structure of the unliganded AADC (Fig. 6A), in which the active site cleft where the catechol ring of dopa resides [refer to Fig. 6B (dopa-liganded AADC)] can be seen from the solvent side at the bottom of the concave area formed at the entrance of the active site. Interestingly, the flexible loop Met328*–Asp339* (hereafter asterisks indicate that the residues come from the neighboring subunit), which is not visible in the crystallographic structure of pig AADC (*15*), is expected to exist near the active site. Therefore, we generated the structure of the flexible loop using MOE. The loop forms an arch over the surface of AADC (Fig. 6A), which explains why the peptide bonds are easily attacked by proteases. However, the short chain length of the loop Met328*–Asp339* prevents it from covering the active site cleft where the catechol ring of dopa resides. The structure shows that the residues Ser340*–Asp345* lie across a groove at the surface of AADC, suggesting that this part can be detached from the surface. Accordingly, the region from Met328* to Asp345* (shown in stick in Fig. 6A) was allowed to move, fit into the concave area, and subjected to energy minimization. The resulting structure is shown in Fig. 6B. Asp329* changes the position and its side chain approaches Arg439, forming a salt bridge. A similar salt bridge is formed between Arg334* and Glu421. These salt bridges fix the residues Met328*, Pro330*, Val331*, Tyr332*, and Leu333* at the entrance of the active site, and the hydrophobic side chains of these residues cover the active site cleft. These residues form another wall that surrounds the catechol ring of the substrate. The peptide bonds of the former flexible loop reside in the concave area. Altogether, the structure explains why, on binding of the ligand, the flexible loop undergoes conformational change and escapes the attack of proteases.

Possible Physiological Significance—The above results shows two important findings. First, the apoenzyme of AADC is degraded faster than the holoenzyme *in vivo*. Second, the holoenzyme is more resistant to proteases only in the presence of the ligand in *vitro*. The latter suggests that, in the cells producing catecholamines, the presence of dopa, which is continuously supplied from tyrosine by the action of tyrosine hydroxylase, stabilizes the flexible loop of the holoenzyme but not that of the apoenzyme. The finding that the CD spectra of the apoenzyme and the holoenzyme in the presence of DopaOMe are essentially the same (Fig. 4) suggests that the substrate dopa does not destabilize the global conformation of the apoenzyme compared to the holoenzyme. Accordingly, the apoenzyme and the holoenzyme would be differentiated *in vivo* by the stability of the flexible loop rather than by the global conformation of the protein, and the apoenzyme would be preferentially degraded. Importantly, this is at present the only plausible mechanism that can explain the differentiation of the apoenzyme from the holoenzyme by the protein-degrading systems. It is, therefore, important to know the extent of saturation of AADC with dopa *in vivo*. Preliminary measurement showed that the concentration of dopa in the PC12 cells is around 20 pmol per μl of the cells. As the cytosol is expected to constitute 50% of the entire cell volume (*27*), the concentration of dopa in the cytosol is expected to be around 40 μM, which is of the same order as the K_m value of AADC for dopa (*6*). If this is the actual concentration of dopa, then the rate of degradation of the apoenzyme is only 2-fold higher than that of the holoenzyme. In order to explain the more than 20-fold higher degradation rate of the apoenzyme, we must investigate further the saturation of AADC with dopa, including subcellular compartmentation of dopa.

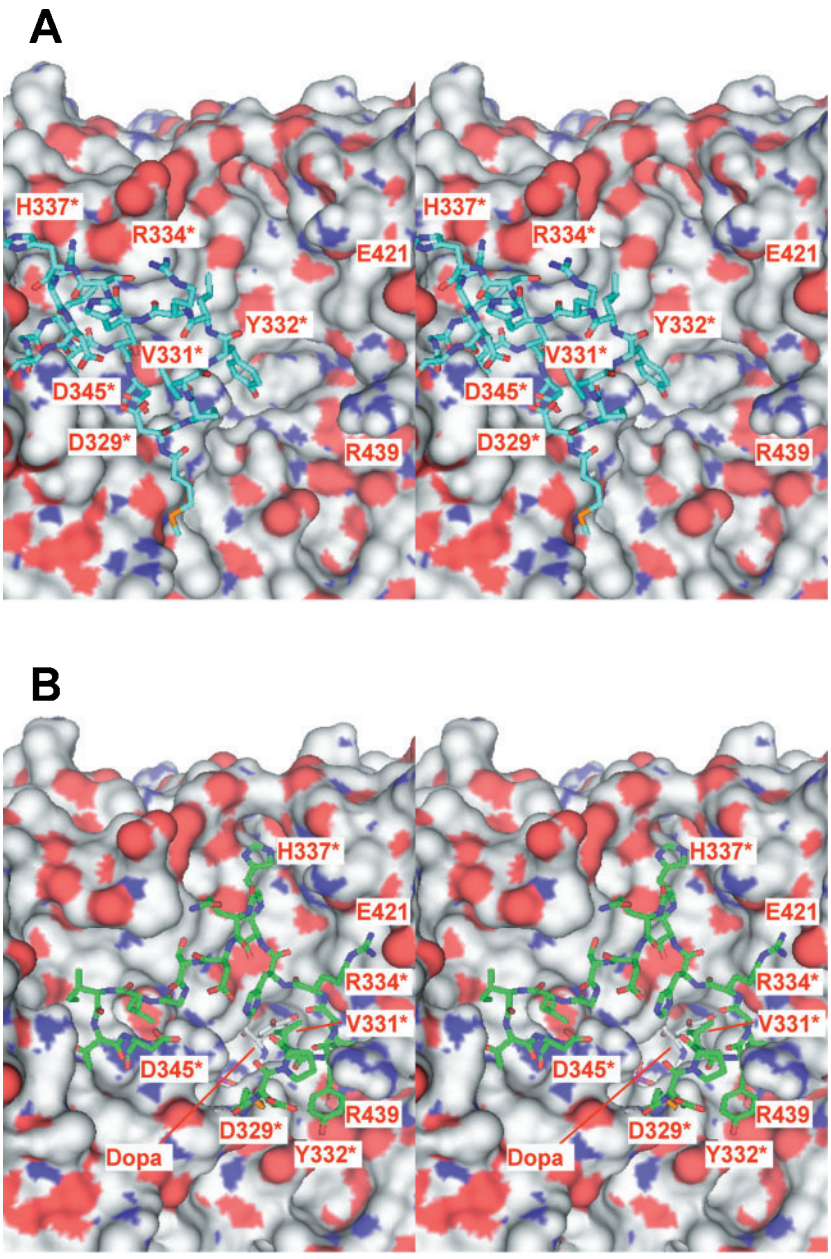

Fig. 6. **(A) Stereo view (parallel) of the proposed structure of rat AADC modeled on the crystal structure of pig AADC.** Homology modeling was carried out using MOE. The residues Met328*–Asp345* are shown in stick model. The other residues are shown in molecular surface model. Red and blue colors show oxygen and nitrogen atoms, respectively. **(B) A model which shows the flexible loop can fit into the concave area at the entrance of the active site.** PLP–dopa and the residues Met328*–Asp345* are shown in stick model. See text for details.

The finding that the apoenzyme is preferentially removed from the cell raises interesting questions. Since there is no clear evidence that the AADC apoenzyme has toxic properties, it is difficult to understand the physiological significance of the dependency of the protein stability on PLP. On the other hand, the dependency on dopa seems to be meaningful if we combine the recent findings on the role of catechol compounds in the pathogenesis of Parkinson's disease. Parkinson's disease is a neurodegenerative disorder characterized by progressive motor dysfunction and the presence of the Lewy body in the substantia nigra (*28*). The Lewy body is a polymerized α-synuclein (fibril), which is formed from the monomeric α-synuclein *via* the oligomeric α-synuclein (protofibril). Recently, it became clear that protofibril, not fibril, is responsible for the pathogenesis of Parkinson's disease, by increasing the permeability of the ER membrane and triggering the Ca^{2+}-mediated cellular pathways that ultimately lead to cell death (*29*). It was found that oxidation products (quinones) of catecholamines (and other catechol compounds) inhibit the conversion of the protofibril to the fibril, probably by reacting with the amino group of α-synuclein and altering the structure required for polymerization (*30*, *31*). Therefore, increasing the intracellular concentration of catechol compounds is considered to accumulate protofibril and promote the pathogenesis of Parkinson's disease. However, as dopamine is sequestrated into synaptic vesicles by the vesicular monoamine transporter while dopa is not (*32*), dopa can be considered to be more toxic to the cell than dopamine. If the conversion of dopa to dopamine is inhibited, the intracellular dopa concentration will be increased and cause neurodegeneration. In this sense, the mechanism by which the

increasing concentration of dopa increases AADC may be a useful device to reduce dopa.

Further studies are required to confirm the above scenario. First, questions on the degradation pathway of AADC, such as which degrading system (lysosomal or proteasomal) is working and whether the cleavage at the flexible loop is the initiation of the degradation pathway, should be answered. The effect of pyridoxine deficiency on the rate of synthesis of AADC (v_{syn} in Fig. 2A) should also be studied. For these issues, the study by Sato (*33*) is of great help. Finally, as described above, the actual degree of AADC saturation with dopa inside the cells should be determined. Studies on these points will provide a more detailed view on the metabolism of the AADC protein in the cells. These studies are now under way in our laboratories.

Note Added in Proof: After submission of this paper for publication, we found a report by Rodríguez-Caso *et al.* that the binding of a suicide substrate α-fluoromethylhistidine to the holo form of histidine decarboxylase, an enzyme structurally and functionally related to AADC, changes the conformation of the enzyme more resistant to denaturation (*34*). The binding is accompanied by a reduction in the Stokes radius, suggesting conformational changes in the subunit interface. This is an important finding that can be compared to our case, in which the flexible loop that covers the active site is considered to be responsible for the stabilization of the enzyme.

We thank Ms. Eriko Matsuo for her excellent technical assistance. This work was supported in part by a grant for Scientific Research on Priority Areas (No. 13125101 to H.H.), and a Grant-in-Aid (No. 13680697 to H.H.) from the Japan Society for the Promotion of Science.

REFERENCES

1. Hayashi, H. (1995) Pyridoxal enzymes: Mechanistic diversity and uniformity. *J. Biochem.* **118**, 463–473
2. Guilarte, T.R. (1989) Regional changes in the concentrations of glutamate, glycine, taurine, and GABA in the vitamin B-6 deficient developing rat brain: association with neonatal seizures. *Neurochem Res.* **14**, 889–897
3. Dakshinamurti, K., Singer, W.D., and Paterson, J.A. (1987) Effect of pyridoxine deficiency in the neuronally mature rat. *Int. J. Vitam. Nutr. Res.* **57**, 161–167
4. Masse, P.G., Vuilleumier, J.P., and Weiser, H. (1991) Aspartate aminotransferase activity in experimentally induced asymptomatic vitamin B_6 deficiency in chicks. *Ann. Nutr. Metab.* **35**, 25–33
5. Katunuma, N., Kominami, E., and Kominami, S. (1971) A new enzyme that specifically inactivates apo-protein of pyridoxal enzymes. *Biochem. Biophys. Res. Commun.* **45**, 70–75
6. Hayashi, H., Mizuguchi, H., and Kagamiyama, H. (1993) Rat liver aromatic L-amino acid decarboxylase: spectroscopic and kinetic analysis of the coenzyme and reaction intermediates. *Biochemistry* **32**, 812–818
7. Temmerman, W., Dhondt, A., and Vandewoude, K. (1999) Acute isoniazid intoxication: seizures, acidosis and coma. *Acta Clin. Belg.* **54**, 211–216
8. Hayashi, H., Tsukiyama, F., Ishii, S., Mizuguchi, H., and Kagamiyama, H. (1999) Acid-base chemistry of the reaction of aromatic L-amino acid decarboxylase and dopa analyzed by transient and steady-state kinetics: Preferential binding of the substrate with its amino group unprotonated. *Biochemistry* **38**, 15615–15622
9. Bradford, M.M. (1976) A rapid and sensitive method or the quantitation of microgram quantity of protein using the principle of protein–dye binding. *Anal. Biochem.* **72**, 248–254
10. Ishii, S., Mizuguchi, H., Nishino, J., Hayashi, H., and Kagamiyama, H. (1996) Functionally important residues of aromatic L-amino acid decarboxylase probed by sequence alignment and site-directed mutagenesis. *J. Biochem.* **120**, 369–376
11. Laemmli, U.K. (1970) Cleavage of structural proteins during the assembly of the head of bacteriophage T4. *Nature* **227**, 680–685
12. Boomsma, F., van der Hoorn, F.A., and Schalekamp, M.A. (1986) Determination of aromatic L-amino acid decarboxylase in human plasma. *Clin. Chim. Acta* **159**, 173–183
13. Hyland, K. and Clayton, P.T. (1992) Aromatic L-amino acid decarboxylase deficiency: Diagnostic methodology. *Clin. Chem.* **38**, 2405–2410
14. Tsuge, H. (1997) Determination of vitamin B6 vitamers and metabolites in a biological sample. *Methods Enzymol.* **280**, 3–12
15. Burkhard, P., Dominici, P., Borri-Voltattorni, C., Jansonius, J.N., Malashkevich, V.N. (2001) Structural insight into Parkinson's disease treatment from drug-inhibited DOPA decarboxylase. *Nat. Struct. Biol.* **8**, 963–967
16. Guilarte, T.R., Wagner, H.N., Jr, Frost, J.J. (1987) Effects of perinatal vitamin B6 deficiency on dopaminergic neurochemistry. *J Neurochem.* **48**, 432–439
17. O'Leary, M.H. and Baughn, R.L. (1977) Decarboxylation-dependent transamination catalyzed by mammalian 3,4-dihydroxyphenylalanine decarboxylase. *J. Biol. Chem.* **252**, 7168–7173
18. Kawasaki, Y., Hayashi, H., Hatakeyama, K., and Kagamiyama, H. (1992) Evaluation of the holoenzyme content of aromatic L-amino acid decarboxylase in brain and liver tissues. *Biochem. Biophys. Res. Commun.* **186**, 1242–1248
19. Rahman, M.K., Nagatsu, T., Sakurai, T., Hori, S., Abe, M., and Matsuda, M. (1982) Effect of pyridoxal phosphate deficiency on aromatic L-amino acid decarboxylase activity with L-DOPA and L-5-hydroxytryptophan as substrates in rats. *Jpn. J. Pharmacol.* **32**, 803–811
20. Guilarte, T.R. (1989) Effect of vitamin B-6 nutrition on the levels of dopamine, dopamine metabolites, dopa decarboxylase activity, tyrosine, and GABA in the developing rat corpus striatum. *Neurochem Res.* **14**, 571–578
21. Kash, S.F., Johnson, R.S., Tecott, L.H., Noebels, J.L., Mayfield, R.D., Hanahan, D., and Baekkeskov, S. (1997) Epilepsy in mice deficient in the 65-kDa isoform of glutamic acid decarboxylase. *Proc. Natl Acad. Sci. USA* **94**, 14060–14065
22. Minelli, A., Charteris, A.T., Voltattorni, C.B., and John, R.A. (1979) Reactions of DOPA (3, 4-dihydroxyphenylalanine) decarboxylase with DOPA. *Biochem. J.* **183**, 361–368
23. Tancini, B., Dominici, P., Simmaco, M., Schinina, M.E., Barra, D., and Voltattorni, C.B. (1988) Limited tryptic proteolysis of pig kidney 3, 4-dihydroxyphenylalanine decarboxylase. *Arch. Biochem. Biophys.* **260**, 569–576
24. Ishii, S., Hayashi, H., Okamoto, A., and Kagamiyama, H. (1998) Aromatic L-amino acid decarboxylase: Conformational change in the flexible region around Arg334 is required during the transaldimination process. *Protein Sci.* **7**, 1802–1810
25. Kern, A.D., Oliveira, M.A., Coffino, P., and Hackert, M.L. (1999) Structure of mammalian ornithine decarboxylase at 1.6 Å resolution: stereochemical implications of PLP-dependent amino acid decarboxylases. *Structure Fold Des.* **7**, 567–581
26. Cheong, C.G., Escalante-Semerena, J.C., Rayment, I. (2002) Structural studies of the L-threonine-*O*-3-phosphate decarboxylase (CobD) enzyme from *Salmonella enterica*: the apo, substrate, and product-aldimine complexes. *Biochemistry* **23**, 9079–9089
27. Alberts, B., Johnson, A., Lewis, J., Raff, M., Roberts K., and Walter, P. (2002) *Molecular Biology of the Cell*, 4th ed., Garland Science Publishing, NewYork
28. Mouradian, M.M (2002) Recent advances in the genetics and pathogenesis of Parkinson disease. *Neurology* **58**, 179–185

29. Volles, M.J. and Lansbury, Jr., P.T. (2002) Vesicle permeabilization by protofibrillar α-synuclein is sensitive to Parkinson's disease-linked mutations and occurs by a pore-like mechanism. *Biochemistry* **41**, 4595–4602
30. Conway, K.A, Rochet, J.C., Bieganski, R.M., and Lansbury, Jr., P.T. (2001) Kinetic stabilization of the α-synuclein protofibril by a dopamine–α-synuclein adduct. *Science* **294**, 1346–1349
31. Shimura, H., Schlossmacher, M.G., Hattori, N., Frosch, M.P., Trockenbacher, A., Schneider, R., Mizuno, Y., Kosik, K.S., and Selkoe, D.J. (2001) Ubiquitination of a new form of α-synuclein by parkin from human brain: Implications for Parkinson's disease. *Science* **293**, 263–269
32. Weingarten, P. and Zhou, Q.Y. (2001) Protection of intracellular dopamine cytotoxicity by dopamine disposition and metabolism factors. *J. Neurochem.* **77**, 776–785
33. Sato, A., Nishioka, M., Awata, S., Nakayama, K., Okada, M., Horiuchi, S., Okabe, N., Sassa, T., Oka, and T., and Natori, Y. (1996) Vitamin B_6 deficiency accelerates metabolic turnover of cystathionase in rat liver. *Arch Biochem Biophys.* **330**, 409–413
34. Rodríguez-Caso, C., Rodríguez-Agudo, D., Moya-García, A.A., Fajardo, I., Medina, M.A., Subramaniam, V., and Sánchez-Jiménez, F. (2003) Local changes in the catalytic site of mammalian histidine decarboxylase can affect its global conformation and stability. *Eur. J. Biochem.* **270**, 4376–4387